Current Optics and Photonics
Vol. 4, No. 4, August 2020, pp. 345-352

ISSN: 2508-7266(Print) / ISSN: 2508-7274(Online)
DOI: https://doi.org/10.3807/COPP.2020.4.4.345

Interferometric Snapshot Spectro-ellipsometry: Calibration and Systematic Error Analysis

Vamara Dembele, Inho Choi, Saeid Kheiryzadehkhanghah, Sukhyun Choi, Junho Kim, Cheong Song Kim, and Daesuk Kim*

Division of Mechanical System Engineering, Jeonbuk National University, Jeonju 54896, Korea

(Received February 5, 2020 : revised April 14, 2020 : accepted April 21, 2020)

We describe a calibration method to improve the accuracy of interferometric snapshot spectroscopic ellipsometry employing a dual-spectrometer sensor scheme. Conventional spectral wavelength calibration of a spectrometer has been performed by using a calibration lamp having multiple peaks at specific wavelength. This paper shows that such a conventional spectrometer calibration method is inappropriate for the proposed interferometric snapshot spectroscopic ellipsometry to obtain highly accurate ellipsometric phase information. And also, systematic error analysis of interferometric snapshot spectroscopic ellipsometry is conducted experimentally.

Keywords : Ellipsometry, Thin-film, Polarization calibration, Interferometry
OCIS codes : (120.2130) Ellipsometry and Polarimetry; (120.3180) Interferometry; (120.5050) Phase measurement; (120.5410) Polarimetry; (120.6200) Spectrometers and spectroscopic instrumentation

I. INTRODUCTION

With the expansion of the application areas of spectroscopic ellipsometry (SE), its performance enhancement has been strongly demanded to fully utilize its advantageous features [1-5]. A conventional SE scheme, however, requires a sequence of consecutive multiple measurements, thus making it impractical for real-time dynamic applications. Moreover, it employs either mechanically or electrically active elements, resulting in complicated and cumbersome systems, although it can provide extremely high precision measurement capability [6, 7]. To improve such speed limitations, various types of snapshot ellipsometry including spectroscopic ellipsometry based on interferometric techniques have been suggested for the last 40 years [8-18]. Although some of those attempts at snapshot spectroscopic ellipsometry based on an interferometric approach have opened a new possibility of commercial uses [10], most interferometric approaches suggested so far still have not met the precision and accuracy level required to compete with conventional high precision SE. The accuracy and precision of SE measurements should match strict requirements for routine process monitoring and control in the modern manufacturing industry. This requires a thorough study of all possible errors such as tool, process and environmentally induced errors.

Recently, our group has proposed a novel snapshot SE scheme based on dual spectrometers by which spectral ellipsometric phase $\Delta(k)$ can be extracted [16]. The proposed snapshot SE solution based on a dual channel scheme can measure the spectral ellipsometric phase $\Delta(k)$ and can retrieve thickness of thin films in real-time speed. Nevertheless, it suffers from systematic errors caused by optical components and imperfect calibration of spectrometers used for the snapshot SE system. The typical wavelength-calibration procedure for the spectrometer system employs one or multiple lamps with known specific spectral lines to match peak wavelength positions of each spectral line to pixels of the array detector used in the spectrometer [19, 20]. In this paper, we use a Mach-Zehnder type inter-

*Corresponding author: dashi.kim@jbnu.ac.kr, ORCID 0000-0003-2471-2910
Color versions of one or more of the figures in this paper are available online.

ferometric snapshot spectro-ellipsometer system employing a white light source to describe the proposed spectral calibration method of the dual spectrometer module. Ideally, the dual spectrometers used for the interferometric snapshot SE need to be exactly the same. Otherwise, it can cause serious measurement errors. This paper describes why it does and how we can solve this problem by using dual spectrometers calibrated by the multiple peaks generated by the interferometer rather than employing dual spectrometers calibrated by using conventional calibration lamps. The proposed calibration method allows the snapshot SE scheme to work robustly in general environments with external noises such as vibration and air drift since the imperfection of the dual spectrometers is one of the critical factors by which the accuracy of the spectroscopic ellipsometric phase $\Delta(k)$ is determined. And also, overall systematic errors of interferometric snapshot spectroscopic ellipsometry are experimentally analyzed in-detail. This paper is organized as follows: firstly, the principle of the interferometric snapshot spectro-ellipsometer is described and why the imperfection of the dual spectrometers can cause a serious systematic problem in the proposed system. After specifying the corrections that must be made in the treatment of the spectrum, we comment on our experimental results.

II. METHODOLOGY

2.1. Experimental Configuration

The experimental system [16] used in this paper is shown schematically in Fig. 1. The system includes: a collimating light source module, an interferometric polarization-modulation module, and a dual spectrum sensing module. A white light from a Tungsten-Halogen lamp is collected into an optical fiber and collimated by a collimation lens, and then it passes through a linear polarizer. The linearly polarized beam hits the measured object sample and the reflected beam enters the specially designed Mach-Zehnder interferometer. The beams from the two arms of the interferometer are recombined and form an interference signal. Finally, the polarized interference signal enters the dual spectrum sensing module and then it is transferred to the dual spectrometers via two multimode optical fibers.

2.2. Measurement Principle

The optical path difference between the two arms of the Mach-Zehnder interferometer is set to around 50 μm, and it creates an interfered signal with high spectral carrier frequency used for extracting the spectral ellipsometric phase information. The measured dual spectra acquired by the dual spectrum sensing module for a thin film of SiO_2 as an object can be described as follows [16]:

$$\begin{aligned} I_p^{SiO_2}(k_p) &= (E_D^x + E_M^x)(E_D^x + E_M^x)^* \\ &= \left|E_D^x\right|^2 + \left|E_M^x\right|^2 + 2\gamma_p \left|E_D^x\right|\left|E_M^x\right|\cos(\Phi_p^{SiO_2}), \end{aligned} \tag{1}$$

where $\Phi_p^{SiO_2} = k_p z_0 + [\delta_p^{SiO_2} - \delta_s^{SiO_2}] + [\eta - \xi] + \varphi_p$.

And

$$\begin{aligned} I_s^{SiO_2}(k_s) &= (E_D^y + E_M^y)(E_D^y + E_M^y)^* \\ &= \left|E_D^y\right|^2 + \left|E_M^y\right|^2 + 2\gamma_s \left|E_D^y\right|\left|E_M^y\right|\cos(\Phi_s^{SiO_2}), \end{aligned} \tag{2}$$

where $\Phi_s^{SiO_2} = k_s z_0 + \varphi_s$.

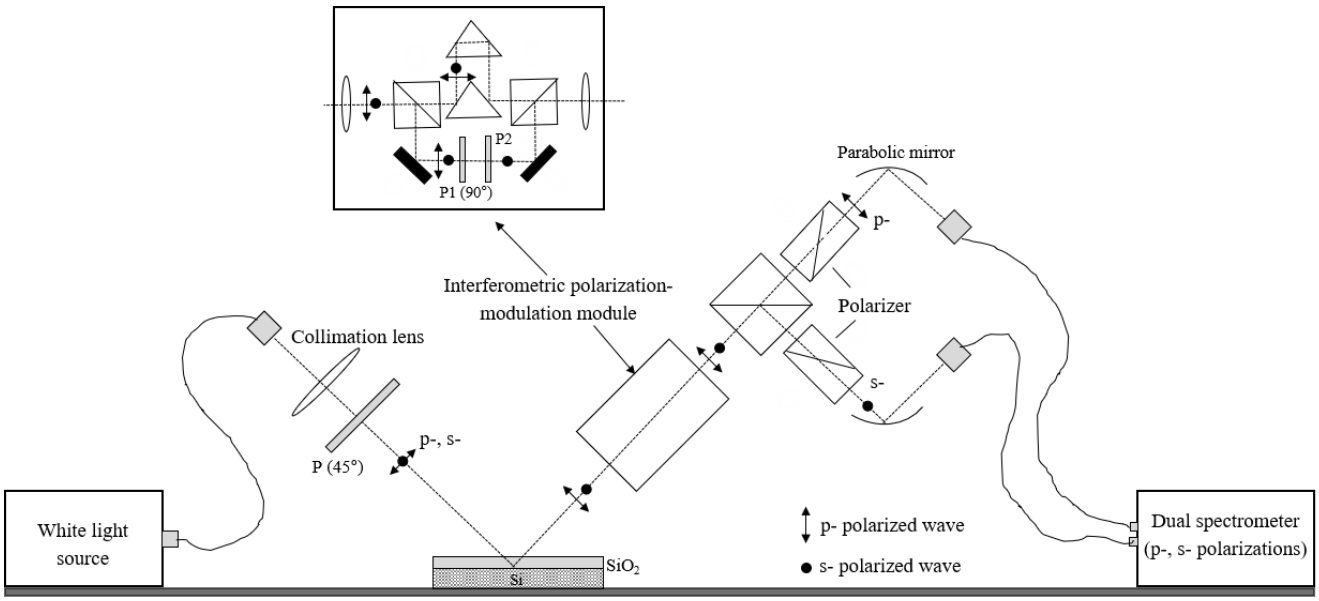

FIG. 1. Schematic representation of the interferometric snapshot spectro-ellipsometer.

Here, $k_{p,s}$ is a wavenumber defined by $2\pi/\lambda_{p,s}$ for p- and s- spectrometer channels. The p- and s-polarized waves are oriented along x-and y-axis. $E_D(k)$ and $E_M(k)$ represent complex waves traveling through a direct path where no polarization modulation occurs and a modulation path with two linear polarizers, respectively. $\gamma_p(k)$ and $\gamma_s(k)$ represent spectral coherence functions of each sensing channel, respectively. The term $z_0 = z_D - z_M$ depicts optical path difference between the two arms of the modified Mach-Zehnder interferometer. η and ξ represent unknown phase of light waves in x- and y-axis, respectively. $\delta_{p,s}^{SiO2}$ denotes the phase changes which have occurred due to the reflection from the thin film object at each sensing channel. $\phi_{p,s}$ signifies unknown additional phase shift terms generated by the spectral interferometric polarization-modulation module used simultaneously for the p- and s- spectral polarization channels, respectively.

Once the two spectra $I_p^{SiO2}(k)$ and $I_s^{SiO2}(k)$ are recorded by the dual spectrum sensing module, we can calculate the total phase functions $\Phi_p^{SiO2}(k)$ and $\Phi_s^{Si02}(k)$, by using the Fourier transform method in the spectral domain [21, 22]. We have applied the same procedures described in [16], which can provide the spectral phase difference between p- and s-polarization $\Delta^{SiO2}(k)$ of a thin-film object as follows:

$$\begin{aligned}\Delta^{SiO_2}(k_p,k_s) &= \Phi_p^{SiO_2}(k_p) - \Phi_s^{SiO_2}(k_s) \\ &= [(k_p - k_s)z_0] + [\delta_p^{SiO_2} - \delta_s^{SiO_2}] + [\eta - \xi] + [\varphi_p - \varphi_s] \\ &= \Delta_{Spectrometer} + \Delta_{Object} + \Delta_{Ligth\_source} + \Delta_{Optics}.\end{aligned} \tag{3}$$

The spectral ellipsometric phase difference $\Delta^{SiO2}(k)$ represented in Eq. (3) contains four terms: $\Delta_{Spectrometer}$ representing the ellipsometric phase uncertainty caused by the imperfect pixel to wavelength calibration of the dual spectrometers, Δ_{Object} meaning the ellipsometric phase information of the measured object which is what we want to extract eventually, Δ_{Light_source} containing ellipsometric phase uncertainty that can be induced by the instability of the light source, and Δ_{Optics} corresponding to ellipsometric phase uncertainty related to the characteristics of optical components employed in the entire system. Note that these all four terms are functions of wavenumber (i.e. wavelength).

III. SPECTRAL CALIBRATION METHOD AND ERROR ANALYSIS

To improve the quality of the measurement and to use it for numerous practical applications, it is important to evaluate all possible uncertainties linked to the entire measurement system including detail measurement procedures. As pointed out in Eq. (3), strict correction of the systematic errors that can be generated by various factors should be made for highly precise and accurate measurements. In this section, we analyze various systematic error sources of the interferometric snapshot spectroscopic ellipsometer system, and end up with one very critical requirement on spectral calibration of the dual spectrometers.

3.1. Influence of the Light Source and Random Error Evaluation

It is well known that random error can be decreased by using an averaging technique. Typical random errors in most interferometer systems are generated by external noise sources such as vibration, air turbulences and instability of light source. We have conducted some experiments to analyse the influence of the white light source as the proposed system handles polarization which might be affected by instability of the light source. A statistical treatment has been carried out to investigate the influence of the light source by acquiring 1000 raw signals within one hour consecutively. Figure 2 shows the stability of the light source at a specific wavelength $\lambda = 560.077$ nm ($k = 11.26\ \mu m^{-1}$). The random noise level of the interfered signal can be decreased to around 0.2% of the main signal by applying averaging of around 20 times.

As depicted in Fig. 2, after certain amount of stabilization time of the light source, the interfered light intensity remains almost constant during the acquisitions of the signals. This confirms that the proposed interferometric snapshot SE system behaves normally as a snapshot system since it shows it is highly robust to external vibration, even in general environments, without using any vibration-free optical table.

3.2. Systematic Errors Evaluation

3.2.1. Dual-spectrometer calibration

All commercial spectrometer systems calibrated by spectrometer manufacturers are not calibrated perfectly as all array sensor-based palm type spectrometers have discrete pixel to wavelength matching. Generally, the wavelength

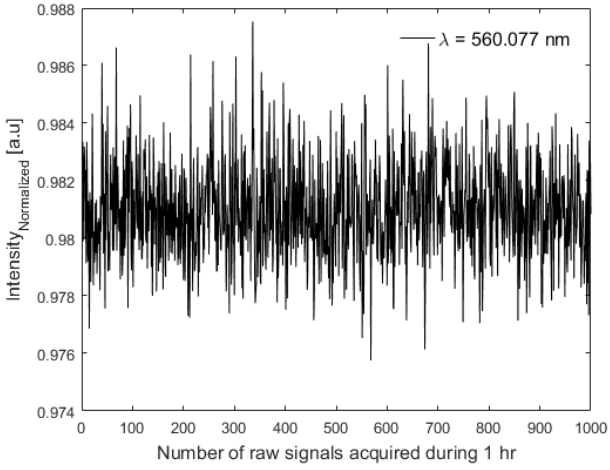

FIG. 2. Light source stability evaluation.

of each spectrometer channel of the proposed system can be written as

$$\lambda_{p,s} = \lambda_R + \delta\lambda_{p,s} . \quad (4)$$

Here, λ_R denotes the real wavelength, $\delta\lambda_p$ and $\delta\lambda_s$ represent the wavelength error due to pixel to wavelength mismatching for p- and s- spectroscopic sensing channels, respectively. As described in Eq. (3) as $\Delta_{Spectrometer}$, the

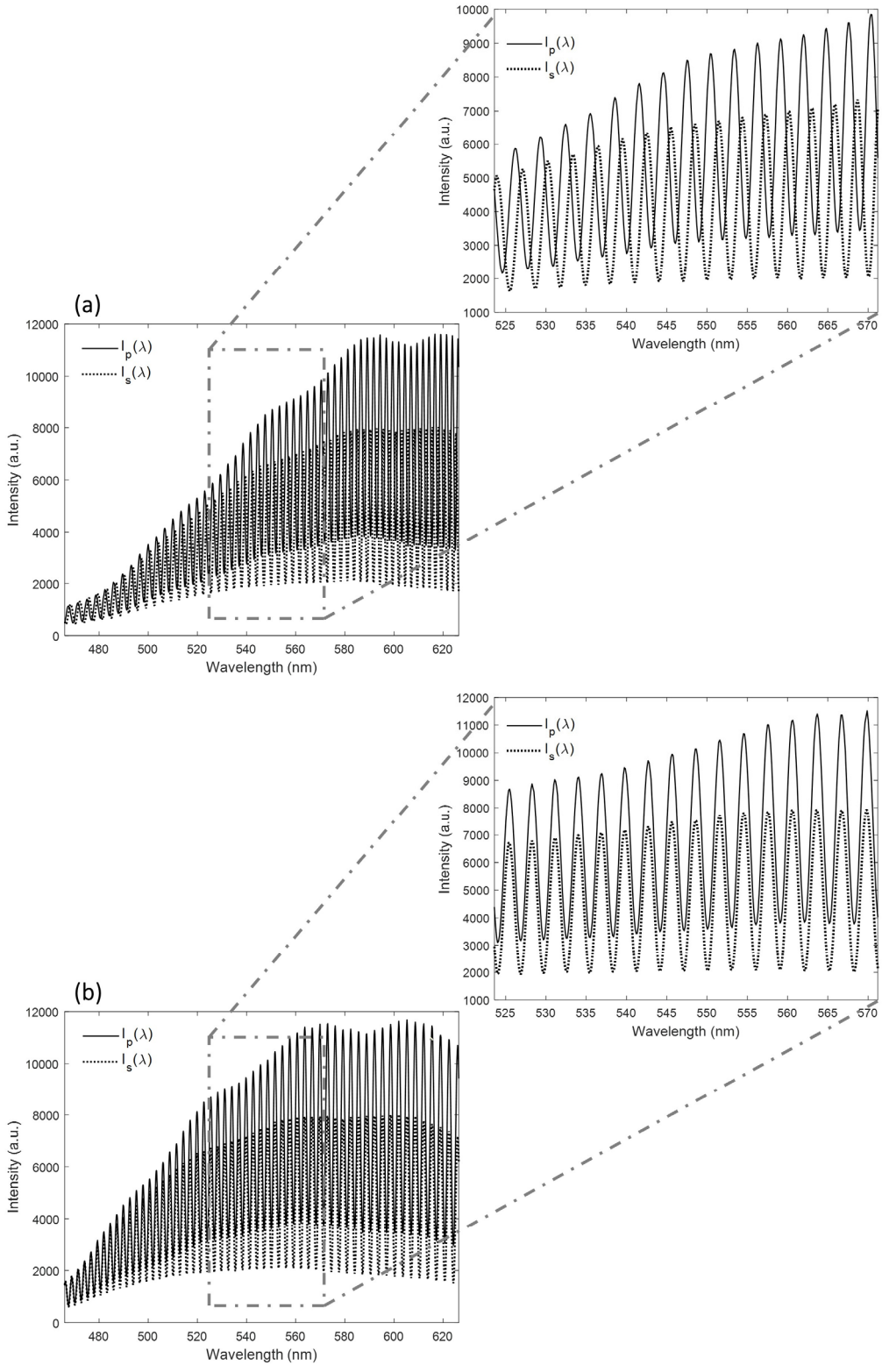

FIG. 3. Interfered spectrum of a dual spectrometer: (a) before spectral calibration and (b) after spectral calibration.

unwanted pixel to wavelength mismatching of the dual spectrometer channels can generate systematic error in measuring the spectral ellipsometric phase Δ_{Object} of the measured thin film object. Although it is not possible to match each pixel to absolute real wavelength, we can make the dual spectrometers have the same peaks in wavelengths by using an interpolation technique. As the interfered signals that can be obtained from the dual spectroscopic channels have a few tens of consecutive multiple peaks due to spectral carrier frequency, we can calibrate the dual spectrometers much more precisely throughout the entire spectral range than the calibration lamp based conventional spectrometer calibration approach. Figures 3(a) and 3(b) show the interfered dual spectra before and after the calibration based on the interpolation process, respectively. We assume that p-polarization channel is sufficiently well calibrated spectrally by a manufacturer. By using the polynomial regression process, we calibrate each pixel position of the s-polarization channel for the entire wavelength range.

Ideally, the term $\Delta_{spectrometer}$ in Eq. (3) needs to be zero. However, perfect calibration is not possible. The best calibration result performed in this study for the dual-spectrometer calibration is expressed as follows:

$$\begin{aligned}\Delta_{spectrometer} &= s(k)z_0 \\ &= (0.062k^2 + 0.997k - 0.035)z_0 .\end{aligned} \tag{5}$$

Note that $s(k)$ in Eq. (5) represents a systematic parameter which remains fixed without any change although z_0 can be slightly changed during the measurement process. After updating the obtained uncertainty factor after the spectrometer calibration, Eq. (3) can be re-written as

$$\Delta^{SiO_2}(k) = \mathrm{s}(k)z_0 + \Delta_{Object}(k) + \Delta_{Optics}(k) . \tag{6}$$

3.2.2. Calibration of optics

In order to remove the Δ_{Optics} in Eq. (6) corresponding to ellipsometric phase uncertainty related to the unknown polarimetric characteristics of optical components employed in the entire system, a reference measurement step is required. In this study, a Si bare wafer is used as a reference sample, and the measured phase difference between the p- and s-polarization channels of the reference can be written as follows:

$$\begin{aligned}\Delta^{Si}(k) &= \Phi_p^{Si}(k) - \Phi_s^{Si}(k) \\ &= \mathrm{s}(k)z_0' - \varepsilon(k) + [\varphi_p - \varphi_s] .\end{aligned} \tag{7}$$

Here, ε represents the amount of phase difference between p- and s-polarization generated by the Si bare wafer. ε is almost zero for a pure Si bare wafer, but it is not ignorable. Note that ε is zero when we use air as the reference by employing a transmission mode. Eventually, we obtain the final calibrated ellipsometric phase information Δ_{Cal} by subtracting Eq. (7) from the Eq. (6) as follows:

$$\begin{aligned}\Delta_{cal}^{SiO_2}(k) &= \Delta^{SiO_2}(k) - \Delta^{Si}(k) \\ &= [\delta_p^{SiO_2} - \delta_s^{SiO_2}] + \varepsilon(k) + \mathrm{s}(k)(z_0 - z_0') .\end{aligned} \tag{8}$$

Note that the entire calibration steps described are performed just one time as a pre-preparation procedure.

IV. EXPERIMENTS AND DISCUSSIONS

4.1. Experimental Setup

The measuring system has no moving parts and no complicated specially manufactured optical components. As depicted in Fig. 1, a multimode fiber with a diameter of 600 μm collects the white light from the light source (100 W Tungsten-Halogen lamp) covering the spectrum from 300 nm to 2100 nm, and an achromatic lens with a focal length of 75 mm collimates the light. The collimated beam passes through a polarizer oriented at 45 degrees with respect to the plane of incidence so that both *p*- and *s*-polarized components are generated. The beam reflected by a thin film object enters the Mach-Zehnder interferometer employing two cube type non-polarizing beam splitters, two aluminum-coated plane mirrors, two knife-edge right-angle prism mirrors, two linear polarizers oriented at 0 and 45 degrees, respectively. An optical window used for compensating the non-linear effect caused by the two linear polarizers. The optical path difference between the two arms of the Mach-Zehnder interferometer equals around 50 μm and it creates a high spectral carrier frequency signal used for extracting the spectral complex wave information. The interfered wave modulated by the two polarizers enters the dual spectrum sensing module. The dual spectrum sensing module is comprised of a non-polarizing beam splitter, two perpendiculars linearly polarized Glan-Thompson polarizers, two parabolic mirrors with focal length of 50 mm, two multimode optical fibers with diameters of 1000 μm and two 2047-pixel array sensor spectrometers with detection range of 395 nm to 648 nm.

4.2. Experimental Results

The enhancement of the measurement accuracy of the interferometric snapshot SE system has been made by applying the proposed dual-spectrometer calibration method for a SiO_2 thin film object. We have conducted experiments on the accuracy enhancement by measuring the SiO_2 thin film with nominal thickness of 500 nm deposited on a Si substrate. The dual interfered spectra measured without applying the proposed spectral calibration process are depicted in Fig. 4(a). By applying the Fast Fourier transform method, we extract the spectral ellipsometric phase $\Delta^{SiO2}(k)$ in Eq. (3) as illustrated in Fig. 4(b) [21, 22]. The extracted spectral ellipsometric phase in Fig. 4(b) consists

of four phase terms $\Delta_{Spectrometer}$, Δ_{Optics}, Δ_{Light_source} and Δ_{Object} as described in Eq. (3). Note that serious systematic error occurs when we employ the dual-spectrometer module calibrated by a lamp-based conventional spectrometer calibration method as illustrated in Fig. 4(b). We can see that extracted ellipsometric phase of the SiO_2 thin film object has large discrepancy compared with that of a commercial spectroscopic ellipsometer (M2000, J.A. Woollam) with a precision of around 0.05 degree.

In order to remove the uncertainty factor $\Delta_{Spectrometer}$ generated by the pixel to wavelength mismatching of the dual-spectrometer module, we have applied the proposed dual-spectrometer calibration method described in the subsection of 3.2.1. Figures 5(a) and 5(b) depict the dual raw intensity data obtained by using the dual-spectrometer module which has been calibrated by the proposed method for the same SiO_2 thin film object, and the extracted spectral ellipsometric phase described in Eq. (6), respectively. Compared with Fig. 4(b), we obtain much closer result to the commercial SE result by minimizing the uncertainty factor caused by $\Delta_{Spectrometer}$. We emphasize that the experimental results show that the main factor of the uncertainty of the interferometric snapshot SE is $\Delta_{Spectrometer}$ rather than Δ_{Optics} or Δ_{Light_source}.

The systematic uncertainty factor caused by the Δ_{Optics} or Δ_{Light_source} can be removed by the reference ellipsometric phase subtraction step as described in Eq. (8). For this, we need to measure a reference by placing a bare Si wafer at the same position where the SiO_2 thin film is placed as illustrated in Fig. 1. Figure 6 represents the extracted spectral ellipsometric phase of the Si bare wafer used as a reference in this study which can be described as Eq. (7). Figure 6 shows the spectral ellipsometric phase $\Delta^{Si}(k)$ extracted by using the same FFT based signal processing used for extracting $\Delta^{SiO2}(k)$ [21, 22]. The dotted line in Fig. 6 represents ε corresponding to the amount of phase difference between p- and s-polarization generated by the pure Si bare wafer.

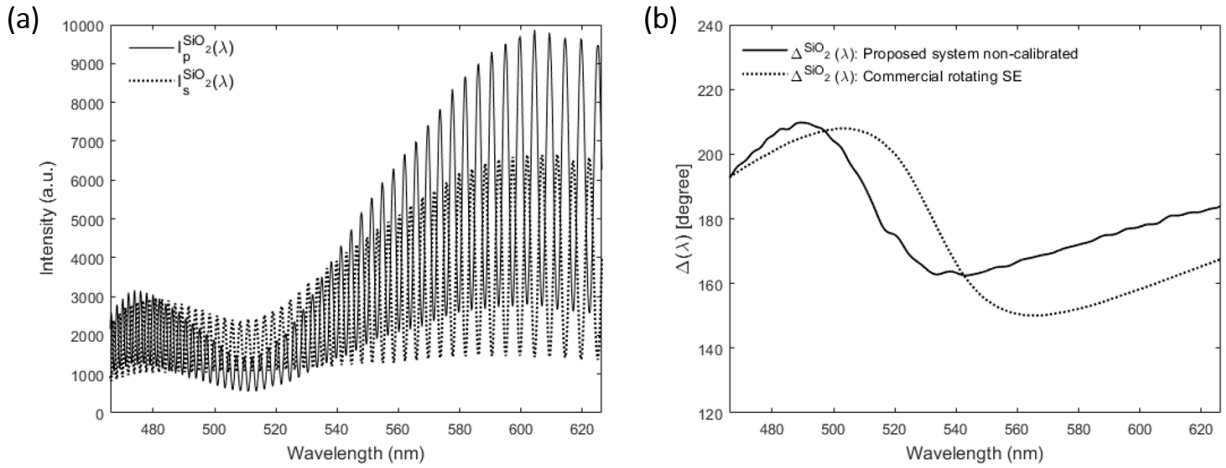

FIG. 4. Non-calibrated dual sensing spectrometer: (a) raw spectral intensity data of a SiO_2 thin film sample with a nominal thickness of 500 nm and (b) the extracted spectral phase difference.

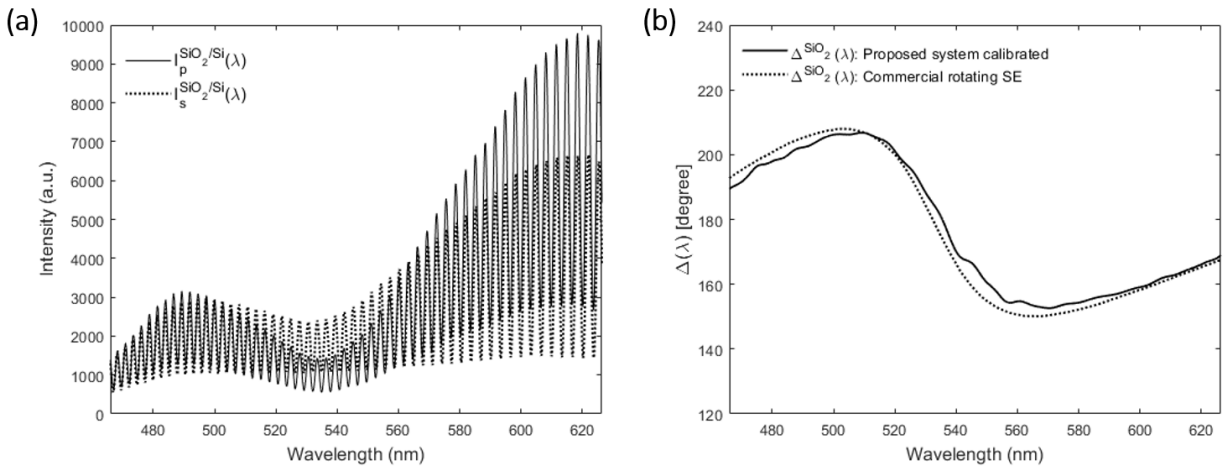

FIG. 5. Calibrated dual sensing spectrometer: (a) raw spectral intensity data of a SiO_2 thin film sample with a nominal thickness of 500 nm and (b) the extracted spectral phase difference.

Since the spectral ellipsometric phase $\Delta^{Si}(k)$ in Fig. 6 contains the two uncertainty terms Δ_{Light_source} and Δ_{Optics}, they can be removed from the spectral ellipsometric phase $\Delta^{SiO2}(k)$ by subtracting the spectral phase of a Si bare wafer $\Delta^{Si}(k)$ to extract the well-calibrated final spectral ellipsometric phase $\Delta_{cal}{}^{SiO2}(k)$ in Eq. (8) as illustrated in Fig. 7. Figure 7 shows the final ellipsometric phase of the thin film $\Delta_{cal}{}^{SiO2}(k)$ (solid line) has a good agreement with that obtained by using a commercial spectro-ellipsometer (dotted line).

As illustrated in Fig. 7, a highly accurate measurement result has been obtained by using the proposed rigorous calibration process although some slight discrepancy exists mainly due to the signal processing performed in the spectral Fourier-domain. This paper describes how important it is to calibrate the dual spectrometers as precisely as possible to minimize the pixel to wavelength mismatching of the dual-spectrometers. The proposed calibration method allows the interferometric snapshot SE scheme to provide an accurate measurement capability in general environments since the imperfectness of the dual-spectrometer calibration can cause a serious systematic uncertainty problem. We expect the proposed dual-spectrometer calibration method based on multiple peaks generated by the embedded interferometer can be extended for various other high precision spectral calibration of spectrometer systems, especially when we want to employ multiple spectrometers for ellipsometric phase measurement applications.

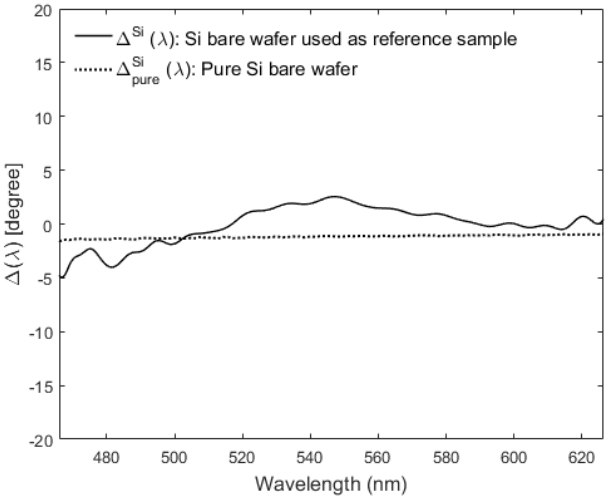

FIG. 6. Spectral phase difference of a Si bare wafer. Solid dark lines represent the extracted $\Delta^{Si}(k)$ of a Si bare wafer used in the proposed system as reference sample. The dotted lines represent the $\Delta_{pure}{}^{Si}(k)$ of a pure Si bare wafer.

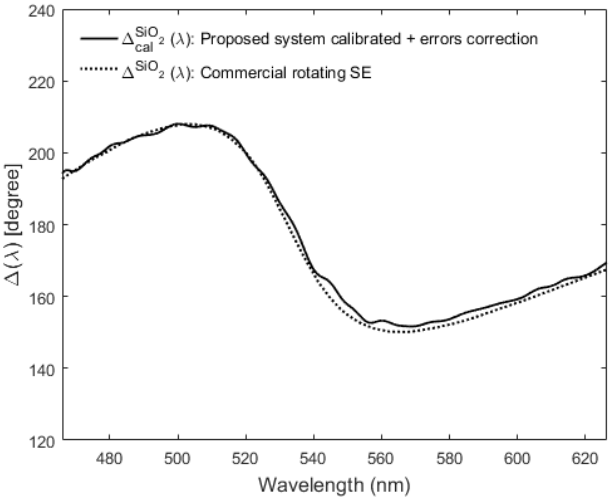

FIG. 7. The extracted $\Delta_{cal}{}^{SiO2}(k)$ of a SiO_2 thin film sample after spectral calibration and systematic errors correction.

V. CONCLUSION

In this paper, a detailed and rigorous calibration method to improve the accuracy of the interferometric snapshot spectroscopic ellipsometry based on dual-spectrometer scheme has been described theoretically, and has been proved experimentally. This paper claims the importance of dual-spectrometer calibration, and also we show how sensitively the pixel-to-wavelength between spectrometers can affect the final systematic uncertainty of the spectral phase measurement system. Eventually, however, we have proved that we can deal with polarization information in spectral domain very precisely. We anticipate that the uncertainty analysis procedures discussed in this work will be very useful in designing other interferometric spectroscopic polarization measurement systems.

ACKNOWLEDGMENT

This work was supported by the National Research Foundation of Korea (NRF) grant funded by the Korean government (NRF-2019R1A2C1010009).

REFERENCES

1. K. Riedling, *Ellipsometry for Industrial Applications* (Springer-Verlag, Wien, 1988).
2. H. G. Tompkins and W. A. McGahan, *Spectroscopic Ellipsometry and Reflectometry: A user's Guide* (Wiley, NY, 1999).
3. D. Aspnes, "Expanding horizons: new developments in ellipsometry and polarimetry," Thin Solid Films **455-456**, 3-13 (2004).
4. A. Dejneka, I. Aulika, V. Trepakov, J. Krepelka, L. Jastrabik, Z. Hubicka, and A. Lynnyk, "Spectroscopic ellipsometry applied to phase transitions in solids: possibilities and limitations," Opt. Express **17**, 14322-14338 (2009).
5. J. W. Weber, V. E. Calado, and M. C. M. Van de Sanden, "Optical constants of graphene measured by spectroscopic ellipsometry," Appl. Phys. Lett. **97**, 091904 (2010).

6. D. E. Aspnes, "Fourier transform detection system for rotating-analyzer ellipsometers," Opt. Commun. **8**, 222-225 (1973).
7. H. Fujiwara, *Spectroscopic Ellipsometry: Principles and Applications* (John Wiley & Sons, England, 2007).
8. H. F. Hazebroek and A. A. Holscher, "Interferometric ellipsometry," J. Phys. E: Sci. Instrum. **6**, 822 (1973).
9. C.-H. Lin, C. Chou, and K.-S. Chang, "Real time interferometric ellipsometry with optical heterodyne and phase lock-in techniques," Appl. Opt. **29**, 5159-5162 (1990).
10. K. Oka and T. Kato, "Static spectroscopic ellipsometer based on optical frequency-domain interferometry," Proc. SPIE **4481**, 137-140 (2002).
11. P. Hlubina, D. Ciprian, and J. Lunacek, "Spectral interferometric techniques to measure the ellipsometric phase of a thin-film structure," Opt. Lett. **34**, 2661-2663 (2009).
12. L. R. Watkins, "Interferometric ellipsometer," Appl. Opt. **47**, 2998-3001 (2008).
13. D. Kim, M. Jin, W. Chegal, J. Lee, and R. Magnusson, "Calibration of a snapshot phase-resolved polarization-sensitive spectral reflectometer," Opt. Lett. **38**, 4829-4832 (2013).
14. D. Kim, Y. Seo, Y. Yoon, V. Dembele, J. W. Yoon, K. J. Lee, and R. Magnusson, "Robust snapshot interferometric spectropolarimetry," Opt. Lett. **41**, 2318-2321 (2016).
15. V. Dembele, M. Jin, B. J. Baek, and D. Kim, "Dynamic spectro-polarimetry based on a modified Michelson interferometric scheme," Opt. Express **24**, 14419-14428 (2016).
16. V. Dembele, M. Jin, I. Choi, W. Chegal, and D. Kim, "Interferometric snapshot spectro-ellipsometry," Opt. Express **26**, 1333-1341 (2018).
17. D. Kim and V. Dembele, "One-piece polarizing interferometer for ultrafast spectroscopic polarimetry," Sci. Rep. **9**, 5978 (2019).
18. V. Dembele, S. Choi, W. Chegal, I. Choi, M. J. Paul, J. Kim, and D. Kim, "Dynamic spectroscopic ellipsometry based on a one-piece polarizing interferometric scheme," Opt. Commun. **454**, 124426 (2020).
19. W. G. Henry and M. R. Meharry. "Calibration of a prism spectrometer," J. Opt. Soc. Am. **51**, 356-359 (1961).
20. C.-H. Tseng, J. F. Ford, C. K. Mann, and T. J. Vickers, "Wavelength Calibration of a Multichannel Spectrometer," Appl. Spectrosc. **47**, 1808-1813 (1993).
21. M. Takeda, H. Ina, and S. Kobayashi, "Fourier-transform method of fringe-pattern analysis for computer-based topography and interferometry," J. Opt. Soc. Am. **72**, 156-160 (1982).
22. D. Kim, S. Kim, H. J. Kong, and Y. Lee, "Measurement of the thickness profile of a transparent thin film deposited upon a pattern structure with an acousto-optic tunable filter," Opt. Lett. **27**, 1893-1895 (2002).